MOOSE Project Part 2

Hongsup Oh

1 Project Overview and Problem Definition

In MOOSE Project Part 2, we need to revise the input file from MOOSE Project Part 1 based on the feedback. Similar to MOOSE Project Part 1, we need to analyze heat transfer in a fuel system consisting of the fuel pellet, gap, and cladding. However, this time, we must account for the coolant conditions around the cladding surface, and the domain dimensionality has changed. The fuel pellet has a radius of 0.5 cm, the gap is 0.005 cm thick, the cladding is 0.1 cm thick, and all components have a height of 100 cm, as shown in Figure 1. In Project 1, the merge block was used to combine the subdomains of the fuel pellet, gap, and cladding; however, it is not necessary and has been removed.

(a) Whole domain of fuel pin. (b) Enlarged section of fuel pin

Figure 1: Fuel Pin Domain: (a) Whole Domain, (b) Enlarged Section.

The strong form of the governing equation to be solved in this project is given by:

$$\rho c_p \frac{\partial T(\mathbf{x})}{\partial t} = \nabla \cdot (k \nabla T(\mathbf{x})) + \dot{q}, \quad \mathbf{x} \in \Omega. \tag{1}$$

The Neumann boundary condition is:

$$-k \nabla T(\mathbf{x}) = h_c (T(\mathbf{x}) - T_\infty), \quad \mathbf{x} \in \partial\Omega_q. \tag{2}$$

where ρ $[kg/m^3]$ represents the mass density, c_p $[J/kg - K]$ is the specific heat capacity, k $[W/m - K]$ denotes the thermal conductivity and h_c $[W/m^2 - K]$ is the convective heat transfer coefficient. In the MOOSE framework, Equation 1 must be transformed into its weak form, and a residual function must be formulated to obtain the temperature field (T) by minimizing Equation 3.

$$r(T) = \int_\Omega \psi_i \rho c_p \frac{\partial T}{\partial t} d\Omega + \int_\Omega \nabla \psi_i \cdot k \nabla T d\Omega - \int_\Omega \psi_i \dot{q} d\Omega + \int_\Gamma \psi_i h_c (T - T_\infty) d\Gamma_q \tag{3}$$

Equation 3 can be represented by Equation 4 where $(\cdot)_\Omega$ denotes the kernel and $< \cdot >_\Gamma$ represents the boundary condition [2, 3]:

$$r(T) = \left(\psi_i, \rho c_p \frac{\partial T}{\partial t}\right)_\Omega + (\nabla\psi_i, k\nabla T)_\Omega - (\psi_i, \dot{q})_\Omega - \langle \psi_i, h_c(T - T_\infty)\rangle_{\Gamma_q} \tag{4}$$

Equation 3 is solved using a nonlinear solver, such as the Newton method, which includes both direct and iterative methods. The detailed procedure of the nonlinear solver is omitted, as it is discussed in the Project 1 report.

Similar to Project 1, the primary objective of this project is to create an input file. Most of the input blocks are the same as in Project 1, with the exception of the Neumann boundary condition block, which is required to account for the convective heat flux condition.

The project report focuses on presenting the results from MOOSE and is structured into five sections: convective heat transfer coefficient calculation, thermal conductivity as a function of temperature, Axial distribution of LHR and ambient temperature, results, and conclusion.

2 Convective heat transfer coefficient calculation

Convective heat transfer coefficient, h_c, is defined as following equation:

$$h_c = \frac{k \cdot Nu}{D_h} \tag{5}$$

where k is the thermal conductivity of the coolant, Nu is the Nusselt number, and D_e is hydraulic diameter. The reactor is assumed to be a PWR channel, with fuel pins arranged in a square lattice configuration, as shown in Figure 2. Additionally, the coolant flow is assumed to be laminar, with a constant uniform heat flux between the coolant and the cladding surface.

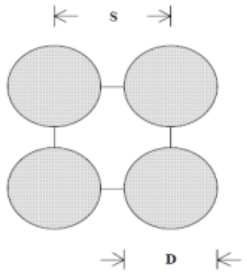

Figure 2: A square lattice configuration.

Considering the given assumptions, the properties are as follows:

$$k = 0.6\ [W/m - K]$$

$$Nu = 4.36$$

The hydraulic diameter D_h is calculated as:

$$D_h = \frac{4A_x}{P_w} = \frac{4(s^2 - \pi D^2/4)}{\pi D} = \frac{4(0.01081^2 - \pi 0.0121^2/4)}{\pi 0.0121} = 0.000218\ [m]$$

The convective heat transfer coefficient, h_c, can be calculated as follows:

$$h_c = \frac{k \cdot Nu}{D_h} = \frac{0.6 \cdot 4.36}{0.000218} = 12000\ [W/m^2 - K]$$

In the project, $h_c = 1.2\ [w/cm^2 - K]$ is used for the Neumann boundary condition.

3 Thermal Conductivity as a Function of Temperature

In this project, a temperature-dependent thermal conductivity model is employed for the diffusion kernel. The fuel pellet is assumed to be UO2, with its thermal conductivity defined as:

$$k_p(T) = \frac{1}{\frac{158}{T} + 0.019T} \quad [W/cm - K] \tag{6}$$

Equation 6 is taken from Fink and Petri (1997) [1]. The gap between the pellet and cladding is assumed to be filled with helium (He), and its thermal conductivity is given by:

$$k_g(T) = 4.68e-4 + 3.81e-6T - 6.79e-10T^2 \quad [W/cm - K] \tag{7}$$

Lastly, the cladding material is assumed to be zirconium (Zr), with its thermal conductivity expressed as:

$$k_c(T) = 0.1098 + 1.4e-4T - 7.44e-8T^2 \quad [W/cm - K] \tag{8}$$

Equations 7 and 8 are taken from Newman, Hansen, and Gaston (2008) [4].

4 Axial distribution of LHR and ambient temperature

The axial distribution of LHR is given by the following equation:

$$LHR(z) = LHR_0 \cdot \sin\left(\frac{\pi(z+\lambda)}{H_e}\right) \quad [W/cm] \tag{9}$$

where $LHR_0 = 350$ $[W/cm]$, λ is is extrapolation distance, and $H_e = H + 2\lambda$. Considering the boundary conditions of neutron flux in a reactor, the neutron flux is adjusted to become zero slightly outside the fuel boundary, rather than at the fuel boundary itself. This is one of the reasons why the extrapolation distance, λ,is introduced. We assume that the extrapolation distance is 10% of the height of the fuel pin. Equation 9 then becomes:

$$LHR(z) = 350 \cdot \sin\left(\frac{\pi(z+10)}{120}\right) \quad [W/cm] \tag{10}$$

The axial distribution of T_∞ is given by the following equation:

$$T_\infty(z) = T_\infty(0) + \frac{1}{\dot{m}c_p}\int_0^z LHR(z)dz \quad [K] \tag{11}$$

where $T_\infty(0) = 500$ $[K]$, R_f is the radius of the fuel pellet, $\dot{m}$ is $\dot{m}$ is the mass flow rate, and c_p is the specific heat. We assume $\dot{m} = 1.5$ $[kg/s]$ and $c_p = 4180$ $[J/kg - K]$. The integral term in Equation 11 can be written using Equation 10 as:

$$\int_0^z LHR(z)dz = -\frac{42000}{\pi}\left(\cos\left(\frac{\pi(z+10)}{120}\right) - \cos\left(\frac{\pi}{12}\right)\right) \tag{12}$$

Equation 11 then becomes:

$$T_\infty(z) = 500 - \frac{42000}{20900\pi}\left(\cos\left(\frac{\pi(z+10)}{120}\right) - \cos\left(\frac{\pi}{12}\right)\right) \quad [K] \tag{13}$$

Equation 10, $LHR(z)$, is used in the heat source kernel, while Equation 13, $T_\infty(z)$, is applied to the convective flux boundary condition.

5 Diffusion kernel for Newton solver

In Project 1, convergence issues arose with the temperature-dependent thermal conductivity case. For the nonlinear solver, the Newton method (direct method) was used instead of PJFNK (iterative method). While the Jacobian matrix is approximately calculated in the PJFNK method, the exact Jacobian matrix is required for the Newton method. The diffusion kernel is defined as follow:

$$R_I = (\nabla\psi_I \cdot k(T)\nabla T^h)_{\Omega_e} \tag{14}$$

where

$$\nabla T^h = \sum_J \nabla\phi_J T_J$$

The Jacobian matrix is built by differentiating R_I with respect to the variable T_J:

$$J_{IJ} = \frac{\partial R_I}{\partial T_J} \tag{15}$$

Using the chain rule, the Jacobian becomes:

$$J_{IJ} = (\nabla\psi_I \cdot k(T)\nabla\phi_J)_{\Omega_e} + \left(\nabla\psi_I \cdot \frac{\partial k(T)}{\partial T_J}\nabla T\right)_{\Omega_e} \tag{16}$$

In Project 1, only the first term of Equation 16 is considered. In the case of constant k, the Jacobian matrix is correct with the first term. However, for the temperature-dependent k, this leads to an incorrect Jacobian matrix. To account for the temperature-dependent thermal conductivity, the term diffusion_coefficient_dT is added to the diffusion kernel. In the material block, additional terms are included to differentiate the temperature-dependent thermal conductivity for the pellet, gap, and cladding. The following equations represent the derivatives of the thermal conductivity with respect to temperature for each material:
For the pellet:

$$\frac{\partial T_p(T)}{\partial T} = \frac{158/T^2 - 0.019}{(158/T + 0.019T)^2} \tag{17}$$

For the gap:

$$\frac{\partial T_g(T)}{\partial T} = 3.81e-6 - 1.358e-9T \tag{18}$$

For the cladding:

$$\frac{\partial T_c(T)}{\partial T} = 1.4e-4 - 1.488e-7T \tag{19}$$

6 Result

Before obtaining the result, a convergence study is conducted to ensure an appropriate mesh. In this study, the number of nodes in the x-direction is fixed at 300, while the number of nodes in the y-direction varies from 10 to 250. The results are shown in Figure 3, where T_{max} represents the maximum temperature along the centerline, and n_y denotes the number of nodes in the y-direction. For n_y = 10 to 100, T_{max} decreases significantly, with noticeable fluctuations. T_{max} converges to 1125.1 at ny = 125 and remains unchanged thereafter. To ensure accurate results, n_y is chosen as 250 for the following calculations. The obtained temperature field is shown in Figure 4. Due to the real scale of the fuel pin, it is difficult to observe the temperature field trend clearly. Therefore, Figure 4 presents an enlarged view in the r-direction, generated using the Python Matplotlib library. Figure 4 shows that the centerline exhibits high temperatures at the core and its surrounding area. Additionally, there is a sudden drop in temperature beyond the gap. To observe the detailed trend, temperature profiles for the pellet centerline, pellet surface, and cladding surface are extracted from

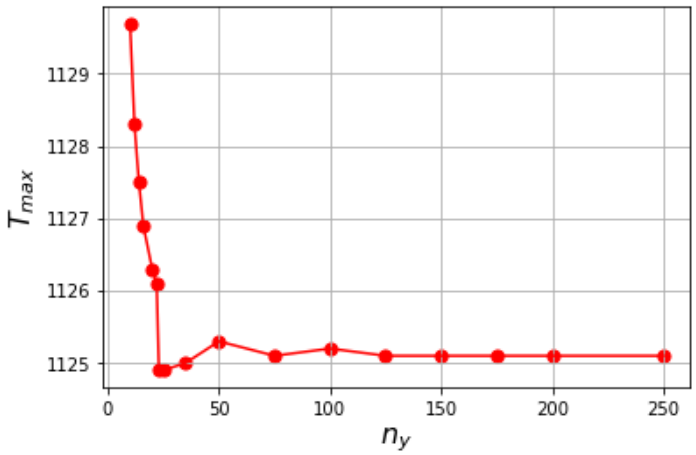

Figure 3: Mesh convergence study

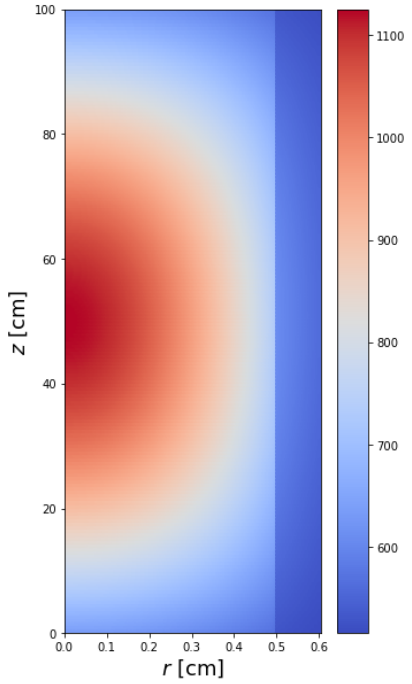

Figure 4: Temperature distribution

Figure 4. Figure 5a presents all three profiles together, with the centerline in blue, the pellet surface in red, and the cladding surface in orange. The x-axis represents the height of the fuel pin, and the y-axis represents the temperature. Figure 5a clearly shows that the center of the fuel pin exhibits the highest temperature. The overall temperature distribution is highest at the centerline, followed by the pellet surface and the cladding surface, with the temperature gradient being steepest at the centerline. Figure 5b shows the trend of each profile. In all cases, the peak temperature occurs around the center of the fuel pin, and the temperature distribution appears symmetric. However, as moving from the centerline to the cladding surface, the symmetry is lost, and the temperature at the top of the fuel pin is slightly higher than at the bottom. The asymmetric profile is caused by the ambient

temperature distribution, as described in Equation 13. If the coefficient of the cosine term in Equation 13 increases, the temperature difference between the top and bottom of the fuel becomes larger, making the asymmetry more pronounced. To assess the degree of asymmetry in all profiles, the location of

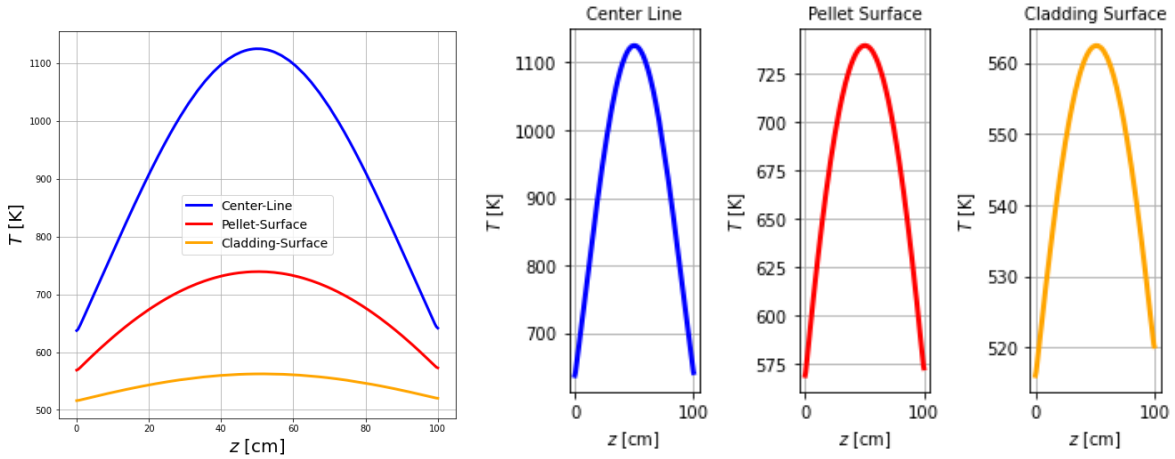

(a) One plot for three temperature profiles.

(b) Separated plots for three temperature profiles.

Figure 5: Temperature profile for fuel center line (blue), pellet surface (red), and cladding surface (orange).

T_{max} is determined using the Python NumPy library. For the centerline, $T_{max} = 1125.1$ $[K]$ occurs at 49.9 $[cm]$, or the pellet surface, $T_{max} = 739.36$ $[K]$ occurs at 50.2 $[cm]$, and for the cladding surface, $T_{max} = 562.39$ $[K]$ occurs at 50.8 $[cm]$. The peak temperature location for the centerline is nearly at the middle of the fuel pin, while the peak temperature locations for the pellet and cladding surfaces are slightly above the midpoint.

7 Conclusion

In MOOSE Project 2, thermodynamic problems are solved using temperature-dependent thermal conductivity, with a given axial LHR and ambient temperature distribution. The fuel system properties are determined based on the assumption that the reactor is a pressurized water reactor (PWR). The temperature-dependent thermal conductivities are referenced from existing research [1, 2]. The convergence issue is addressed by incorporating the derivative term of thermal conductivity into the diffusion kernel, and the fluctuating temperature trend is corrected. Unlike Project 1, a mesh convergence study is conducted. The simulation results indicate that the maximum temperature occurs near the middle of the fuel pin. However, the temperature profile is not perfectly symmetric due to the influence of the ambient temperature distribution.

References

[1] JK Fink and MC Petri. Thermophysical properties of uranium dioxide-version 0 for peer review. Technical report, Argonne National Lab.(ANL), Argonne, IL (United States), 1997.

[2] D. Gaston, C. Newman, G. Hansen, and D. Lebrun-Grandie. Moose: A parallel computational framework for coupled systems of nonlinear equations. *Nuclear Engineering and Design*, 239(10):1768–1778, 2009.

[3] Idaho National Laboratory. Moose: Multiphysics object oriented simulation environment, 2024. Accessed: 2024-02-28.

[4] Chris Newman, Glen Hansen, and Derek Gaston. Three dimensional coupled simulation of thermomechanics, heat, and oxygen diffusion in uo2 nuclear fuel rods. *Journal of Nuclear Materials*, 392(1):6–15, 2009.